Combination of Multi-Satellite Altimetry and Shipborne Gravity Data for Geoid Determination in a Coastal Region of Eastern Canada

G.S. Vergos, R.S. Grebenitcharsky and M.G. Sideris

Department of Geomatics engineering, University of Calgary, 2500 University Drive N.W., Calgary, Alberta, Canada, T2N 1N4

ABSTRACT

The combination of satellite altimetry and shipborne gravity data for optimal geoid determination in the region of Newfoundland, Eastern Canada, is investigated and compared with existing geoid solutions in the area under study. In this study, a new high-resolution multi-satellite (GEOSAT-GM, ERS1-GM, T/P) altimetric geoid is computed and validated, and then combined with shipborne gravity data to obtain the final model. The newly released 1998 GEOSAT-GM data referring to JGM-3 will be used, thus higher accuracy is expected. T/P data are used as control points for the resulting geoid, which is then compared to existing geoid solutions (GSD solutions) in the test area. We will also investigate the use of a global Sea Surface Topography (SST) model to test how well it models the stationery part of the SST. We will focus on the use of the Multiple Input Multiple Output System Theory (MIMOST) method for the efficient and optimal combination of heterogeneous data. Finally two geopotential models, namely EGM96 and GPM98b, are implemented to test how well they model the long wavelength part of the geoid.

KEYWORDS

Geoid determination, marine geoid, satellite altimetry, sea surface heights, shipborne gravimetry, sea surface topography, combination, MIMOST.

1. INTRODUCTION

The eastern coast of Canada is an area of extensive research activities relevant to geoid determination and gravity field modelling. The Geodetic Survey Division (GSD) of Natural Resources Canada (NRCan) in collaboration with universities like the ones of Calgary and New Brunswick generate new geoid solutions almost every five years, taking advantage of the new available and more accurate data sets. The specific area under study is very advantageous since it offers a great amount of shipborne gravity data, with very good resolution and coverage close to the coastline, collected during the past decades. This enables us to overcome difficulties and uncertainties of geoid determination close to the coastline. Additionally, since it is a part of the Atlantic Ocean, global models for various gravity field and oceanography related quantities, such as ocean circulation and SST models, can be safely used. As it is well known such models are not generated for closed sea areas, just like the Mediterranean Sea, hence they are not usually used in these cases. With the advent of satellite altimetry a vast amount of high-accuracy and high-resolution data were available for use in gravity field determination. Our study is focused in the Eastern coastal region of Canada ($43^o \leq \varphi \leq 57^o$ and $298^o \leq \lambda \leq 312^o$) including the island of Newfoundland in the Labrador Sea and the St. Lawrence gulf.

In this study we focus, using the well-know remove-restore method, on the combined use of multi-satellite altimetry and shipborne gravity data for a high-accuracy and high-resolution ($3' \times 3'$) marine geoid determination in the area under study. We determine, using the available datasets, purely altimetric and gravimetric geoid solutions and then using the Multiple Input Multiple Output System Theory (MIMOST) (Bendat and Piersol, 1986; Sideris, 1996; Andritsanos et al., 2000a) for the efficient combination of heterogeneous data, we compute the final geoid solutions. We also want to investigate

whether the combined use of satellite altimetry and shipborne gravity data will improve geoid modelling compared to the gravimetric geoid only.

Altimetric Sea Surface Heights (SSHs) from the ERS1 and the newly released (NOAA 1997) GEOSAT Geodetic Missions (GMs) are used for the computation of the altimetric geoid solution. Stacked 3rd year TOPEX/POSEIDON (T/P) SSHs are used as control points for the validation of our solutions. The 3rd year of the T/P mission was selected so that a common observation period between two satellites (T/P and ERS1-GM) would be available. The marine free air gravity anomalies used in this study were kindly provided to us by Mr. M. Véronneau and were generated by the Geological Survey of Canada (Véronneau 2001). The gravimetric geoid was computed by the 1D-FFT Stokes convolution (Haagmans et al., 1993; Sideris and She, 1995) using the available marine free-air gravity anomalies. The above three solutions were referenced to two geopotential models, namely EGM96 (Lemoine et al., 1996), complete to degree and order 360, and GPM98 (Wenzel, 1999), complete to degree and order 1800. For the determination of the Sea Surface Topography (SST) signal we used the model from the simultaneous EGM96 adjustment (Lemoine et al. 1998). As control for our gravimetric geoid solutions the KMS99 global marine gravity field (Andersen and Knudsen 1998) was used. Comparisons with the official Canadian geoid GSD95 (Véronneau 1997) were performed in order to assess the differences with our solutions due to the different reference fields (in the computation of GSD95, OSU91A geopotential model was used as a reference field) and the more accurate data used.

2. ALTIMETRIC GEOID

Almost 73% of our planet's surface is covered by water and contrary to the immense size of water areas our knowledge of the processes taking place in the earth's oceans was little until the late 1970's. With the advent of the space era and the launch of the Seasat altimetric satellite in late 1970's the potentials of satellite altimetry to monitor the oceans became evident. It was the first time that a satellite was put in orbit with its primary goal being the monitoring of the oceans. The satellite managed to collect only 42 hours of data which were though more than that collected during the last 100 years of earth-based observations. Satellite altimetry is an increasing in accuracy method and provides a dense, long-term, repeated in period and accurate monitoring of the earth's oceans. It provides an economical tool, compared to shipborne gravimetry, to model the oceans and determine the gravity field over great water areas. The geodetic missions of GEOSAT and ERS1 altimetric satellites provide a vast amount of data with resolutions of 2-4km in the equator (Smith et al., 1994), which cover the Earth densely and offer precise data sets due to the accurate models used for the geophysical and instrumental corrections and the approximation of the satellite orbit. Because of the improved models used in the processing of altimetry data a marine geoid determination with an accuracy close to a few centimeters is feasible. The altimetric data sets used in this study were GEOSAT-GM newly released SSHs referred to JGM-3 (Joint Gravity Model 3) orbits and were provided by NOAA (1997). The observation period of this data set was from March 30th, 1985 to September 30th, 1986. Additional altimetric data were those of the mapping phase of ERS1-GM SSHs from AVISO (1998). The observation period of these altimetric data extends from April 10th, 1994 to March 21st, 1995. Finally, the 3rd year of T/P SSHs distributed by AVISO (1998) were used. The period of observation of this data set was from October 16th, 1994 to October 8th, 1995.

2.1 VALIDATION OF GEOSAT-GM DATA AND GEOID SOLUTION

An initial preprocessing step in the validation of the GEOSAT-GM SSHs was their correction due to the instrumental and geophysical errors, included in the SSH observations, in order to get corrected SSHs.

The GEOSAT-GM data were provided to us in the usual Geophysical Data Record (GDR) format and the models and methods used for the aforementioned corrections are the same as those described in the GEOSAT-GM handbook (1997). The total number of corrected SSHs available in the area under study were 95348 point values. As a next step we corrected the GEOSAT-GM SSHs for the SST signal. The SST model used in this study comes from the simultaneous EGM96 geopotential model adjustment (Lemoine et al. 1998) and was kindly provided to us by Dr. N. Pavlis. The model comes as a set of spherical harmonic coefficients of the SST complete to degree and order 20. Using the model we computed SST values on the points were GEOSAT-GM SSHs were available and we removed them from the SSHs signal. These SSHs are considered as geoid heights (N). The statistics of the original and corrected for the SST signal GEOSAT-GM SSHs are presented in Table 1.

max	**min**	**mean**	**std**
330.383	-311.601	6.174	±19.206
331.039	-310.989	6.816	±19.310

Table 1. Original and corrected for the SST signal GEOSAT-GM data. Unit: [m].

The available GEOSAT-GM data records cover not only sea but some continental areas as well, thus the first test had to deal with the removal of the continental data. It is well-known that satellite altimetry SSHs give some erroneous values close to the coastline due to the scattering of the radar altimeter pulse from the shallow sea bottom; for that reason, data close to the coastline were removed as well. A 1′×1′ bathymetric model for the area under study was used (Sandwell, 1996) and an interpolation of depth values was carried out at the points where SSHs from GEOSAT-GM were available. Following this interpolation process data points with depths greater than -50m were neglected as suspected to contain blunders. According to this test, 6619 point values (6.94%) were finally removed (see Table 2).

max	**min**	**mean**	**std**
331.039	-310.989	8.849	±17.959

Table 2. GEOSAT-GM data after the bathymetry test. Unit: [m].

From Tables 1 and 2 for the SSHs before and after the bathymetry test some very large minimum and maximum values are still present, thus indicating the presence of outliers. On the other hand we can see an improvement of the standard deviation value at the level of 1.5m. After the bathymetry test the long wavelength part of the geoid heights was removed by subtracting the contribution of EGM96 (Lemoine et al., 1998) and GPM98b (Wenzel, 1998) geopotential models from the SSHs. The statistics of the so derived residual geoid heights (N_{res}) are summarized in Table 3.

	max	**min**	**mean**	**std**
$\mathbf{N_{res}}$ (EGM96)	338.818	-316.654	-1.892	±10.252
$\mathbf{N_{res}}$ (GPM98b)	338.892	-316.768	-2.050	±10.249

Table 3. GEOSAT-GM residual undulations. Unit: [m]

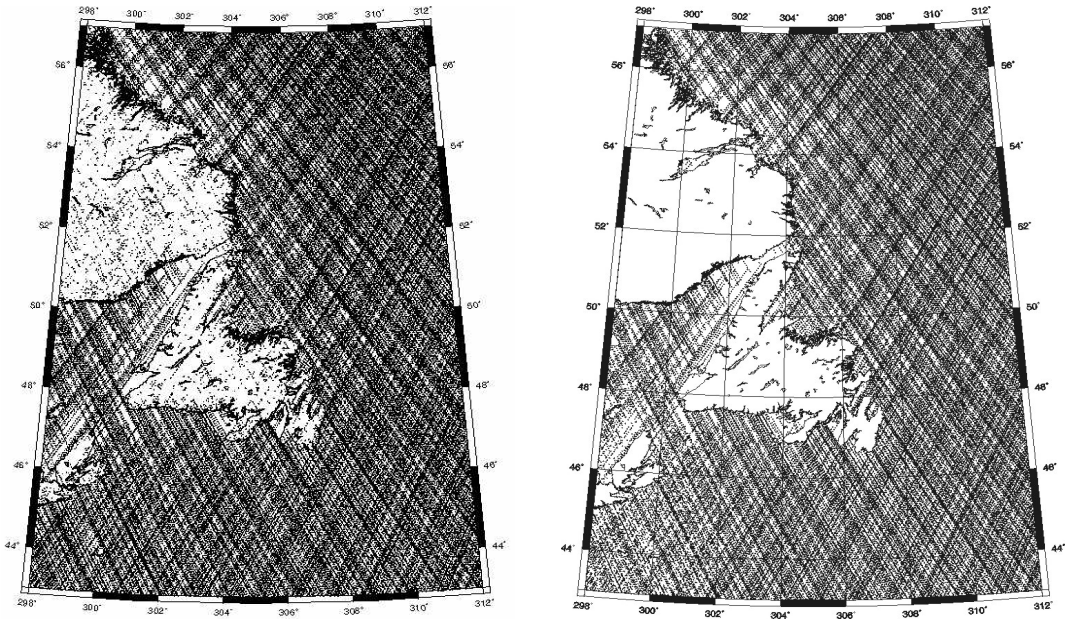

(a) (b)

Figure 1. GEOSAT-GM data distribution before (a) and after (b) the bathymetry test.

The residual geoid heights in Table 3 indicate a number of unexpected values. This is due to the presence of blunders and/or systematic errors. To remove these large values, an additional 3rms test for blunder detection was performed for the GEOSAT-GM residual geoid heights. After the 3rms test 7225 (8.14%) in the case of EGM96 and 10293 (11.6%) in the case of GPM98b residual geoid heights were removed. To summarize, during the two validation tests (bathymetry and 3rms), 13844 GEOSAT-GM data points (14.52%) reduced to EGM96 geopotential model were removed and 16921 data points (17.74%) reduced to GPM98b were eliminated.

The remaining data in the area under study ($43^o \leq \varphi \leq 57^o$ and $298^o \leq \lambda \leq 312^o$) are 81504 and 78427 residual geoid heights referenced to EGM96 and GPM98b respectively. The statistics of these residual geoid heights in the test area are given in Table 4.

	max	**min**	**mean**	**std**
$\mathbf{N_{res}}$ (EGM96)	0.720	-0.721	0.141	±0.195
$\mathbf{N_{res}}$ (GPM98b)	0.581	-0.581	0.010	±0.194

Table 4. GEOSAT-GM residual undulations after the 3rms test. Unit: [m]

To verify the effectiveness of the bathymetry mask and that of the 3rms validation we compare the statistics of the GEOSAT-GM data before and after the tests (Tables 1 and 4 respectively). From these two tables it is evident that the extreme maximum and minimum values are removed and the residual geoid heights, in terms of the standard deviation values, are at the ±19.5cm level. To these residual geoid heights a crossover adjustment was applied for the minimization of the orbital errors. Comparing the residual geoid heights before and after the adjustment insignificant improvement, for the case of EGM96, and deterioration, for the case of GPM98, in terms of the standard deviation and the mean value of the differences was detected. This fact can be mainly attributed to the improved and high accuracy orbits used for the present release of GEOSAT-GM GDRs (JGM3). For this reason, the

residual geoid heights after the 3rms test and before adjustment were used for the subsequent geoid determination.

The point residual geoid heights were interpolated onto a 3′×3′ grid. Then, during the last step of the remove-restore method, the contribution of EGM96 and GPM98b geopotential models to the residual geoid heights was restored and the final geoid height solutions of GEOSAT-GM altimetry data were calculated (see Table 5).

	max	**min**	**mean**	**std**
N (EGM96)	32.480	-20.539	5.918	±13.482
N (GPM98b)	32.481	-20.549	5.925	±13.496

Table 5. The final geoid solution from GEOSAT-GM altimetry data. Unit: [m]

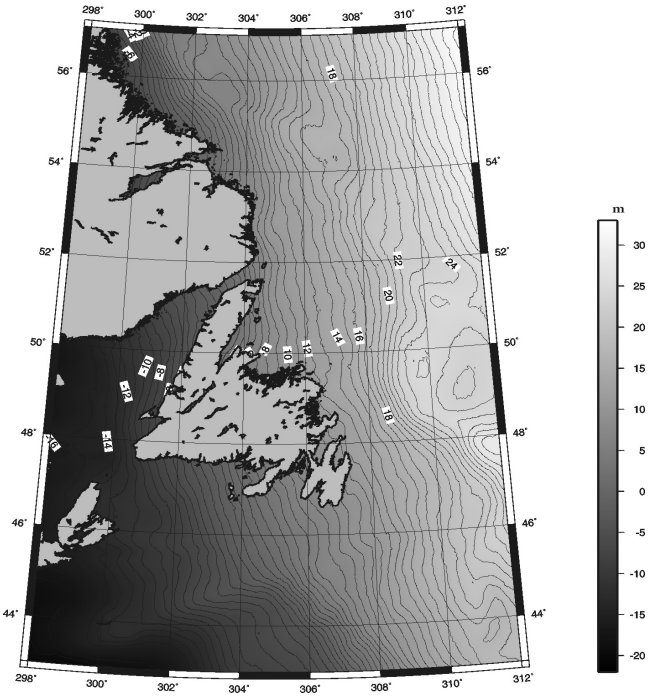

Figure 2. The final geoid solution from GEOSAT-GM to GPM98 reference filed.

2.2 VALIDATION OF ERS1-GM DATA AND GEOID SOLUTION

The ERS1 satellite altimetry SSHs were provided to us in the usual GDR format, thus a first preprocessing step, as in the case of GEOSAT data, for the correction due to the geophysical and instrumental errors was needed. This was done according to the models and methods described in the AVISO handbook (AVISO, 1998) for the ERS1-GM data. A total number of 56053 ERS1-GM corrected SSHs for the area under study were used. ERS1 data do not refer to land or close to the coastline regions hence the bathymetry mask validation test was not needed in this case. Following again the remove-restore method the contribution of the EGM96 and GPM98b geopotential models was removed from the corrected SSHs. The statistics of ERS1-GM residual SSHs are shown in Table 6.

	max	min	mean	std
$\mathbf{SSH_{res}}$ (EGM96)	0.852	-1.459	-0.421	±0.343
$\mathbf{SSH_{res}}$ (GPM98b)	1.203	-2.269	-0.555	±0.347

Table 6. ERS1-GM residual undulations. Unit: [m]

As with the case of GEOSAT-GM data we then removed the signal of the SST. To do so we interpolated, from the spherical harmonics SST model, SST values on the points where ERS1-GM SSHs were available. The statistics of these residual geoid heights are presented in Table 7. From the such derived residual geoid heights and in order to detect the presence of blunders a 3rms test was applied. During this test 500 (0.009%) for EGM96 and 1984 (0.035%) for GPM98b data points were removed. The statistics of the ERS1-GM data after the 3rms test are summarized in Table 8. A crossover adjustment, with the same results as the ones discussed for the case of GEOSAT-GM data, was applied for the ERS1-GM residual geoid heights.

	max	min	mean	std
$\mathbf{N_{res}}$ (EGM96)	1.569	-0.594	0.213	±0.200
$\mathbf{N_{res}}$ (GPM98b)	1.942	-1.527	0.079	±0.257

Table 7. ERS1-GM residual undulations after the correction for the SST signal. Unit: [m]

	max	min	mean	std
$\mathbf{N_{res}}$ (EGM96)	0.831	-0.594	0.205	±0.186
$\mathbf{N_{res}}$ (GPM98b)	0.633	-0.635	0.072	±0.198

Table 8. ERS1-GM residual undulations after the 3rms test. Unit: [m]

Thus, the data after the 3rms test and before the adjustment, were used for the interpolation on a 3′×3′ grid. Finally the contribution of EGM96 and GPM98b geopotential models was restored in these gridded residual geoid heights. The statistics of the final geoid height solutions from ERS1-GM altimetric mission are given in Table 9 and the solution referenced to GPM98b is depicted in Figure 3.

	max	min	mean	std
N (EGM96)	32.440	-20.484	6.019	±13.446
N (GPM98b)	32.457	-20.483	5.992	±13.472

Table 9. The final geoid solution from ERS1-GM altimetry data. Unit: [m]

3. GRAVIMETRIC GEOID

The gravity data used were shipborne free-air gravity anomalies covering the area under study. 160481 marine free-air gravity anomalies for the Labrador Sea and the St. Lawrence gulf were used (Véronneau

2001). The statistics of the gravity data are presented in Table 10 and the data distribution is depicted in Fig. 4.

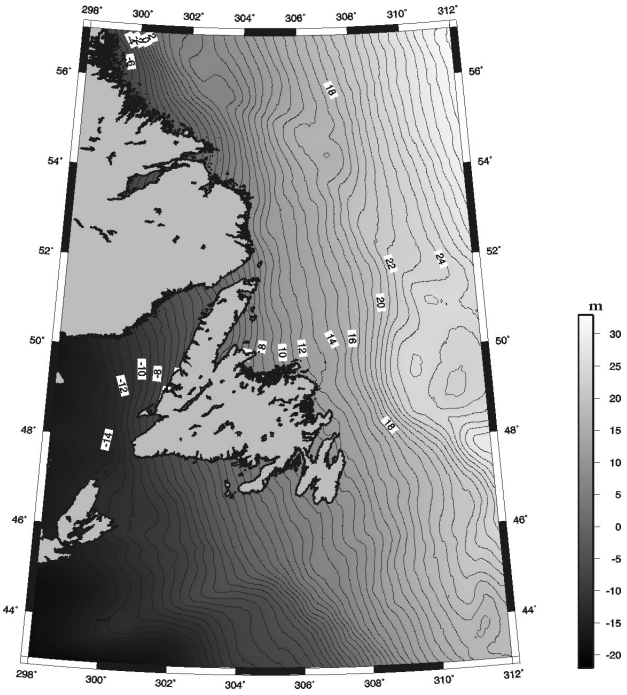

Figure 3. The final geoid solution from ERS1-GM to GPM98reference field.

	max	min	mean	std
Δg	133.900	-103.500	0.249	±31.054

Table 10. Statistics of gravity data. Unit: [mGal]

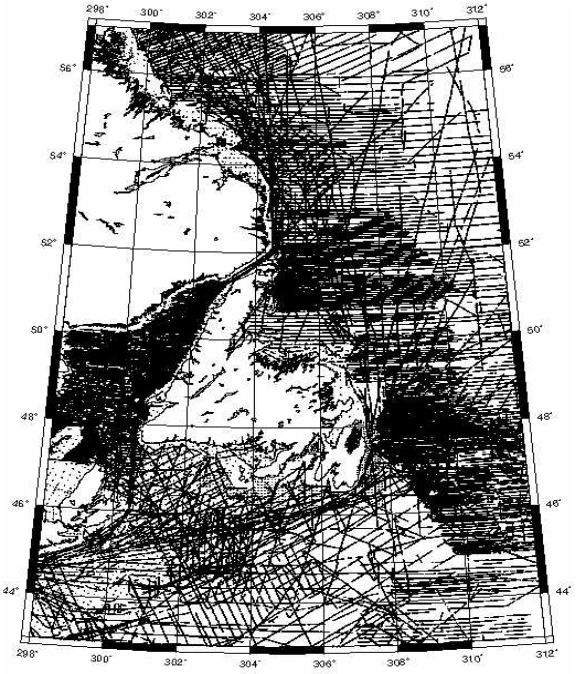

Figure 4. Distribution of gravimetric data.

From Fig. 4 it can be seen that the data distribution is irregular, showing very dense coverage of the St. Lawrence gulf and the eastern part of Newfoundland reaching a resolution of 15′′. On the other hand the data distribution in the southern and north-eastern part of the area under study is sparser reaching a resolution of 6′-7′. For that reason we decided to set the resolution of our final gravimetric geoid solution to 3′×3′ so that it will compensate the sparser distributions and be in agreement with the altimetric solutions previously determined. The data come from shipborne campaigns held during the last 30 years, thus varying in accuracy. They are referenced to GRS67 and since the altimetry data refer to GRS80 a transformation of the available gravity data to GRS80 was needed. Following Li (1996) and Wenzel (1999) the formulas used for the transformation are:

$$\Delta g_{GRS80} = \Delta g_{GRS67} + \gamma_{GRS67} - \gamma_{GRS80} \tag{1}$$

$$\gamma_{GRS67} = 978031.8(1+0.0053024\sin^2\varphi-0.0000059\sin^2(2\varphi)) \tag{2}$$

$$\gamma_{GRS80} = 978032.7(1+0.0053024\sin^2\varphi-0.0000058\sin^2(2\varphi)) \tag{3}$$

The so referenced to GRS80 free-air gravity anomalies were first reduced to EGM96 and GPM98b reference surfaces (Table 11). Then a 3rms test for blunder detection was performed during which 1929 (0.012%) referenced to EGM96 and 2856 (0.019%) referenced to GPM98 residual gravity anomalies were removed (see Table 12). These residual gravity anomalies were gridded on a 3′×3′ grid and the computation of the residual geoid heights was carried out by applying the 1-D FFT spherical Stokes convolution (Haagmans et al, 1993; Sideris and She, 1995).

$$N^{gr} = \frac{R\Delta\varphi\Delta\lambda}{4\pi\gamma}\mathcal{F}_1^{-1}\left\{\sum_{\varphi=\varphi_1}^{\varphi_n}\mathcal{F}_1\{S\}\mathcal{F}_1\{\Delta g\cos\varphi\}\right\} \tag{4}$$

Where N^{gr} is the gravimetric geoid height, R is the mean earth radius, γ is the normal gravity, Δg denotes gravity anomaly, and $S(\psi)$ is Stokes' function. The statistics of these residual geoid heights are reported in Table 13.

	max	**min**	**mean**	**std**
$\mathbf{N_{res}}$ (EGM96)	52.365	-74.653	-3.784	±10.564
$\mathbf{N_{res}}$ (GPM98b)	48.033	-124.605	-3.760	±6.183

Table 11. Statistics of reduced gravity anomalies to EGM96 and GPM98b reference fields. Unit: [mGal]

	max	**min**	**mean**	**std**
$\mathbf{N_{res}}$ (EGM96)	31.287	-31.301	-3.550	±9.812
$\mathbf{N_{res}}$ (GPM98b)	16.675	-17.089	-3.322	±4.628

Table 12. Statistics of reduced gravity anomalies to EGM96 and GPM98b reference fields after the 3rms test. Unit: [mGal]

	max	min	mean	std
$\mathbf{N_{res}}$ (EGM96)	1.315	-1.858	-0.473	±0.293
$\mathbf{N_{res}}$ (GPM98b)	0.344	-0.560	-0.177	±0.116

Table 13. Statistics of residual gravimetric geoid undulations. Unit: [m]

The final gravimetric geoid solutions were then determined following the last step of the remove-restore method by restoring the contribution of the reference models EGM96 and GPM98b to geoid height residuals. The statistics of these solutions are given in Table 14. Finally, we depict the gravimetric geoid height solutions for both reference fields in Figures 5 and 6.

	max	min	mean	std
N (EGM96)	28.730	-22.476	0.299	±13.105
N (GPM98b)	31.893	-20.862	5.709	±13.759

Table 14. The final gravimetric geoid solution to EGM96 and GPM98b reference fields. Unit: [m]

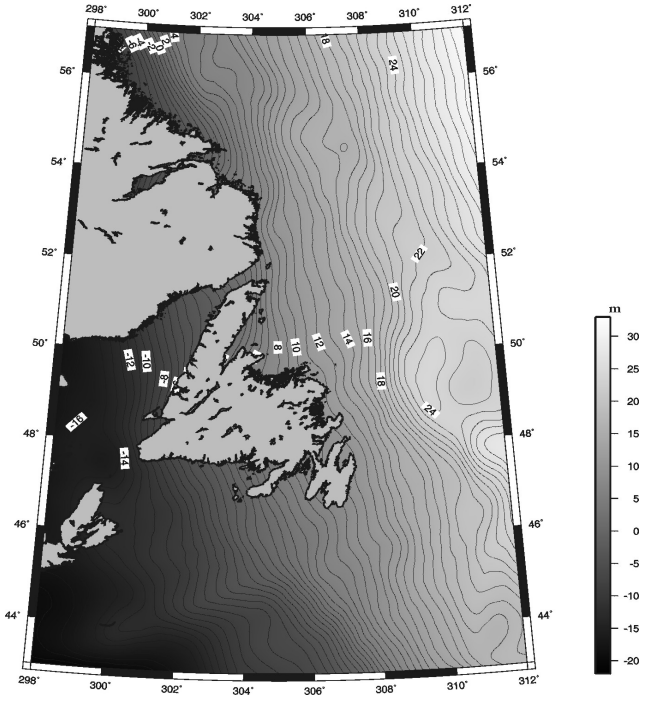

Figure 5. The final gravimetric geoid solution to EGM96 reference field.

4. COMBINED METHOD AND GEOID SOLUTION

Having determined the altimetric and gravimetric geoid height solutions, combined ones were computed using the Multiple Input Multiple Output System Theory (MIMOST) as presented in Andritsanos et al. (2000a), Andritsanos et al. (2000b). The data used for the combination method are the altimetric residual geoid heights from ERS1-GM and GEOSAT-GM reference to EGM96 and GPM98b fields and the corresponding gravimetric residual geoid heights.

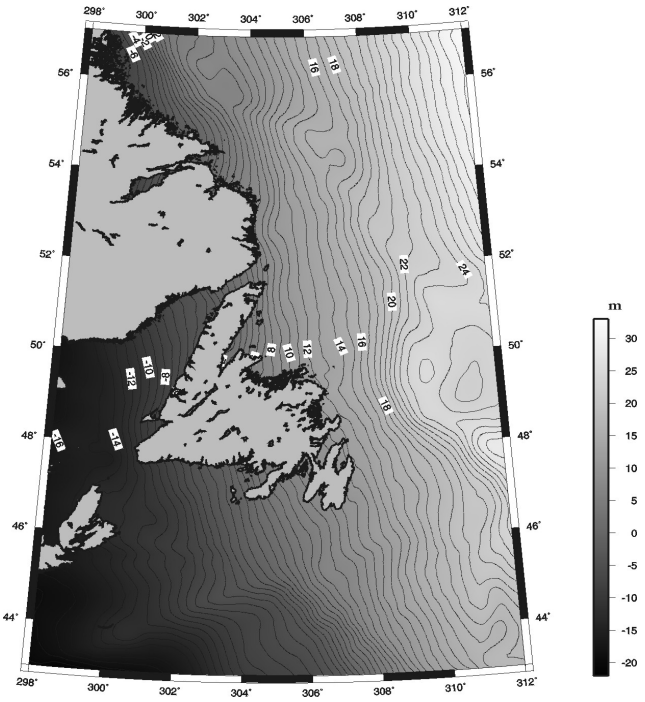

Figure 6. The final gravimetric geoid solution to GPM98 reference field.

Due to the lack of specific information about the errors in both the altimetric and the gravimetric solution, simulated noises were used as input error. Randomly distributed fields (white noise) were generated in MATLAB® using 5cm standard deviation for the altimetry derived geoid heights and 10cm standard deviation for the gravimetric one. The final solution from the combination method, as well as the output error PSD function, were calculated according to the following equations:

$$\hat{N}_o = \begin{bmatrix} H_{\hat{N}N_g} & H_{\hat{N}N_a} \end{bmatrix} \left(\begin{bmatrix} P_{N_{og}N_{og}} & P_{N_{og}N_{oa}} \\ P_{N_{oa}N_{og}} & P_{N_{oa}N_{oa}} \end{bmatrix} - \begin{bmatrix} P_{m_g m_g} & 0 \\ 0 & P_{m_a m_a} \end{bmatrix} \right) \begin{bmatrix} P_{N_{og}N_{og}} & P_{N_{og}N_{oa}} \\ P_{N_{oa}N_{og}} & P_{N_{oa}N_{oa}} \end{bmatrix}^{-1} \begin{bmatrix} N_{og} \\ N_{oa} \end{bmatrix} \tag{5}$$

$$\begin{aligned} P_{\hat{e}\hat{e}} = \Bigg\{ & \begin{bmatrix} H_{\hat{N}N_g} & H_{\hat{N}N_a} \end{bmatrix} \left(\begin{bmatrix} P_{N_{og}N_{og}} & P_{N_{og}N_{oa}} \\ P_{N_{oa}N_{og}} & P_{N_{oa}N_{oa}} \end{bmatrix} - \begin{bmatrix} P_{m_g m_g} & 0 \\ 0 & P_{m_a m_a} \end{bmatrix} \right) - \begin{bmatrix} \hat{H}_{\hat{N}_o N_{og}} & \hat{H}_{\hat{N}_o N_{oa}} \end{bmatrix} \\ & \begin{bmatrix} P_{N_{og}N_{og}} & P_{N_{og}N_{oa}} \\ P_{N_{oa}N_{og}} & P_{N_{oa}N_{oa}} \end{bmatrix} \Bigg\} \left(\begin{bmatrix} H^*_{\hat{N}N_g} \\ H^*_{\hat{N}N_a} \end{bmatrix} - \begin{bmatrix} \hat{H}^*_{\hat{N}_o N_{og}} \\ \hat{H}^*_{\hat{N}_o N_{oa}} \end{bmatrix} \right) + \begin{bmatrix} \hat{H}_{\hat{N}_o N_{og}} & \hat{H}_{\hat{N}_o N_{oa}} \end{bmatrix} \begin{bmatrix} P_{m_g m_g} & 0 \\ 0 & P_{m_a m_a} \end{bmatrix} \begin{bmatrix} H^*_{\hat{N}N_g} \\ H^*_{\hat{N}N_a} \end{bmatrix} \end{aligned} \tag{6}$$

where $\hat{N}_o$ is the spectrum combined geoid solution, N_g and N_a are the spectra of the pure gravimetric and altimetric signals respectively, N_{og} and N_{oa} are the spectra of gravimetric and altimetric observations, m_g and m_a are the input noises, H_{xy} is the theoretical operator that connects the pure input y and output signals x, $\hat{H}_{x_o y_o}$ is the optimum frequency impulse response function, $\hat{e}$ is the output noise and P_{xy} are PSD functions (Andritsanos et al, 2000a). The statistics of the final geoid height solution from the optimal combination of the heterogeneous residual geoid heights referenced to the EGM96 and GPM98b geopotential models can be seen in Table 15 and are depicted in Figure 7.

	max	min	mean	std
N (EGM96)	24.612	-15.809	5.028	±10.175
N (GPM98b)	25.302	-15.625	5.294	±10.368

Table 15. The combined geoid solution to EGM96 and GPM98b reference fields. Unit: [m]

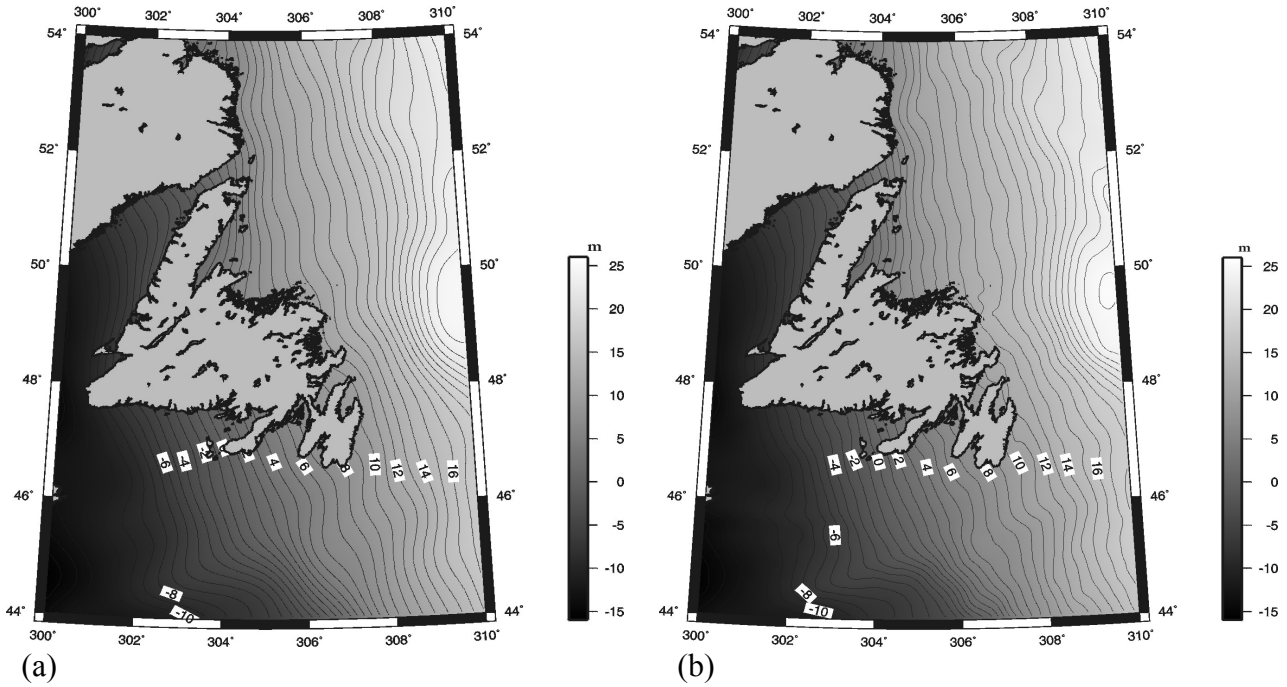

Figure 7. The final geoid height solutions from the MIMOST method for EGM96 (a) and GPM98b (b) reference surfaces.

5. COMPARISON OF THE COMPUTED GEOID HEIGHT SOLUTIONS WITH T/P SSHS, GSD95 AND KMS99

The previously determined geoid height solutions were compared with GSD95, the official geoid of Canada. Especially for the gravimetric solutions we use KMS99 altimetry derived global gravity field for the accuracy assessment. Then we compare our solutions with stacked T/P SSHs from the 3rd year of the satellite mission, which are considered as geoid heights when neglecting the SST signal. T/P SSHs are known for their high accuracy and they can be safely used as control points for our solutions. From Figure 8 we can see that the differences between GSD95 and ERS1-GM, referenced to EGM96, altimetry solution are at the ±26cm level. These differences ($N_{GSD95} - N_{ERS1\text{-}GM}$) present a large minimum value (-2.187cm), which is mainly attributed to the enhanced data used in the ERS1-GM solution and to the different reference fields used, since GSD95 refers to OSU91A. From Figure 9 the differences between the gravimetric geoid solution referenced to EGM96 and KMS99 geoid are at the ±29cm level indicating that our gravimetric geoid is close to the altimetry derived KMS99 one. Still the superiority of altimetry data is evident though.

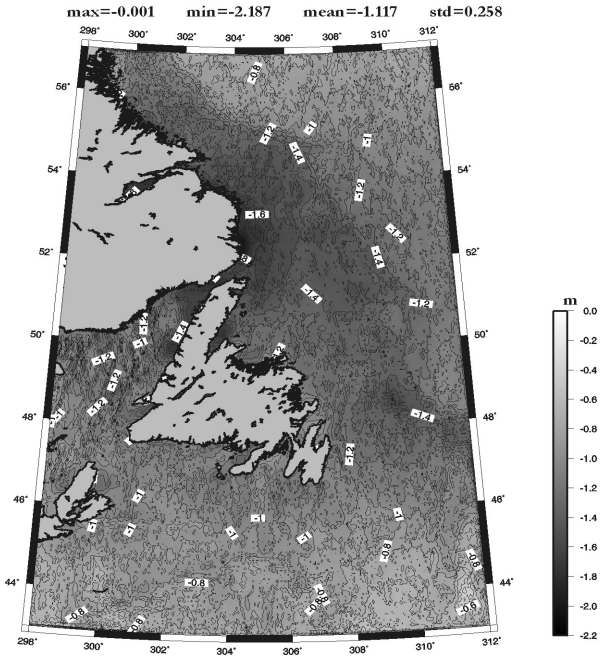

Figure 8. Geoid height differences between GSD95 and ERS1-GM geoid solution to EGM96 reference field.

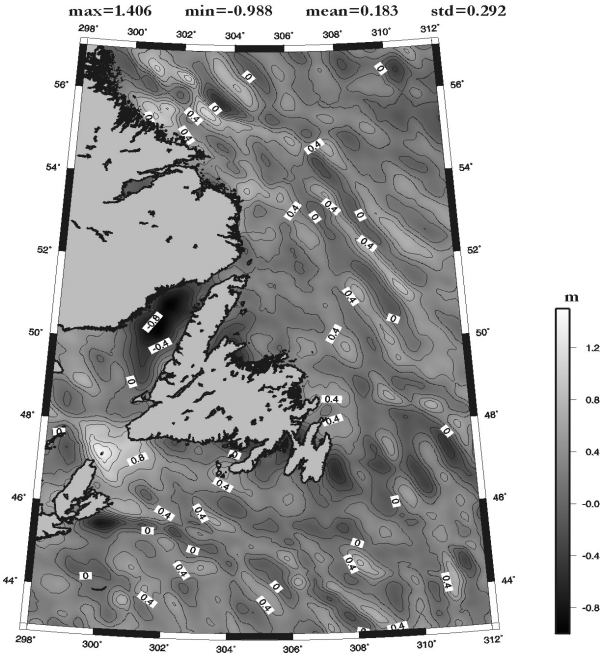

Figure 9. Geoid height differences between KMS99 and gravimetric solution referenced to EGM96 model.

The differences between GSD95 and the geoid solution from the combination method are presented, with their statistics, in Figures 10a and 10b. We can see that the combined use of altimetry and shipborne gravity data improves the agreement with GSD95, especially close to the coastline, and this can be attributed to the fact that the shipborne data were used in the GSD95 geoid modeling as well. Nevertheless the differences due to the different fields used are evident especially in the case of GPM98b where the standard deviation is at the ±50cm level.

For the comparisons between the aforementioned solutions and the stacked SSHs from the 3rd year of the T/P mission the computed differences were minimized by using a four-parameter transformation model:

$$SSH_{T/P} = N - b_o \cos\phi\cos\lambda - b_1 \cos\phi\sin\lambda - b_2 \sin\phi - b_3 \quad (7)$$

where the parameters b_o, b_1, b_2 and b_3 were calculated by the least squares technique and N is the altimetric, gravimetric or combined geoid height depending on the solution under consideration. The statistics of the differences, after bias and tilt fir, between T/P SSHs and the ERS1-GM, GEOSAT-GM and gravimetric solutions, are presented in Tables 16, 17 and 18 respectively.

	max	**min**	**mean**	**std**
$\mathbf{T/P_{SSHs} - N_{EGM96}}$	0.562	-0.574	0.000	±0.095
$\mathbf{T/P_{SSHs} - N_{GPM98b}}$	0.557	-0.481	0.000	±0.094

Table 16. Geoid height differences between T/P SSHs and ERS1-GM altimetric solutions after bias and tilt fit. Unit: [m]

	max	**min**	**mean**	**std**
$\mathbf{T/P_{SSHs} - N_{EGM96}}$	0.858	-0.450	0.000	±0.109
$\mathbf{T/P_{SSHs} - N_{GPM98b}}$	0.840	-0.420	0.000	±0.105

Table 17. Geoid height differences between T/P SSHs and GEOSAT-GM altimetric solutions after bias and tilt fit. Unit: [m]

	max	**min**	**mean**	**std**
$\mathbf{T/P_{SSHs} - N_{EGM96}}$	0.962	-0.895	0.000	±0.253
$\mathbf{T/P_{SSHs} - N_{GPM98b}}$	0.822	-0.797	0.000	±0.222

Table 18. Geoid height differences between T/P SSHs and the gravimetric solutions after bias and tilt fit. Unit: [m]

Comparing the standard deviation of the differences between the different geoid height solutions and the stacked T/P heights, it is easily concluded that the altimetric solutions show better agreement with T/P SSHs compared to the gravimetric ones. The agreement of the pure altimetric geoid heights with T/P SSHs is at the level of ±9 for ERS1-GM and ±10 for GEOSAT-GM. The differences for the gravimetric solutions on the other hand reach the level of ±25cm in terms of the standard deviation value. Comparing the use of the two different reference fields we can conclude that they give almost the same results for the satellite altimetry geoid solutions when for the gravimetric ones the solution to GPM98b gives 3cm better agreement with T/P SSHs.

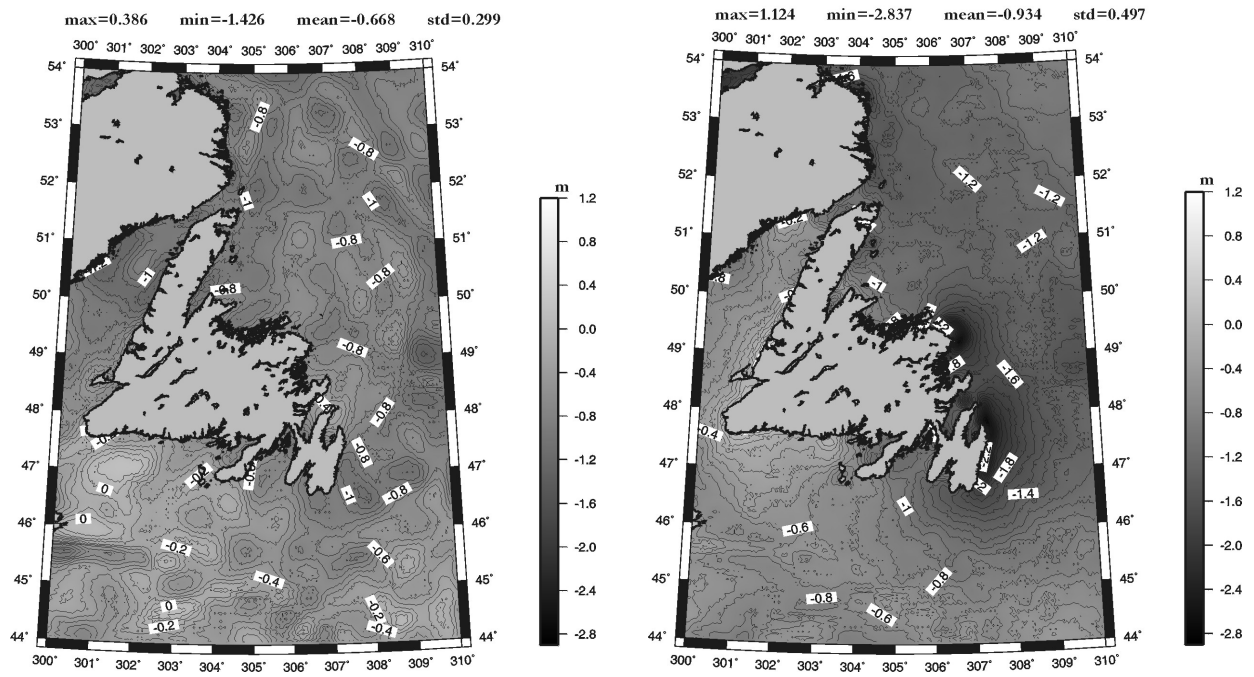

(a) (b)

Figure 10. Geoid height differences between GSD95 and the combined solutions referenced to EGM96 (a) and GPM98b (b) fields.

For the differences between the stacked T/P SSHs with the geoid heights from the optimal combination method an accuracy close to ±22cm and ±20cm in terms of standard deviation of the differences, for EGM96 and GPM98b respectively, is achievable (see Figure 11). Comparing to the same statistics for the gravimetric solutions, we can see that the combined use of satellite altimetry and shipborne gravity data improves the agreement with T/P SSHs by 3cm for both EGM96 and GPM98b.

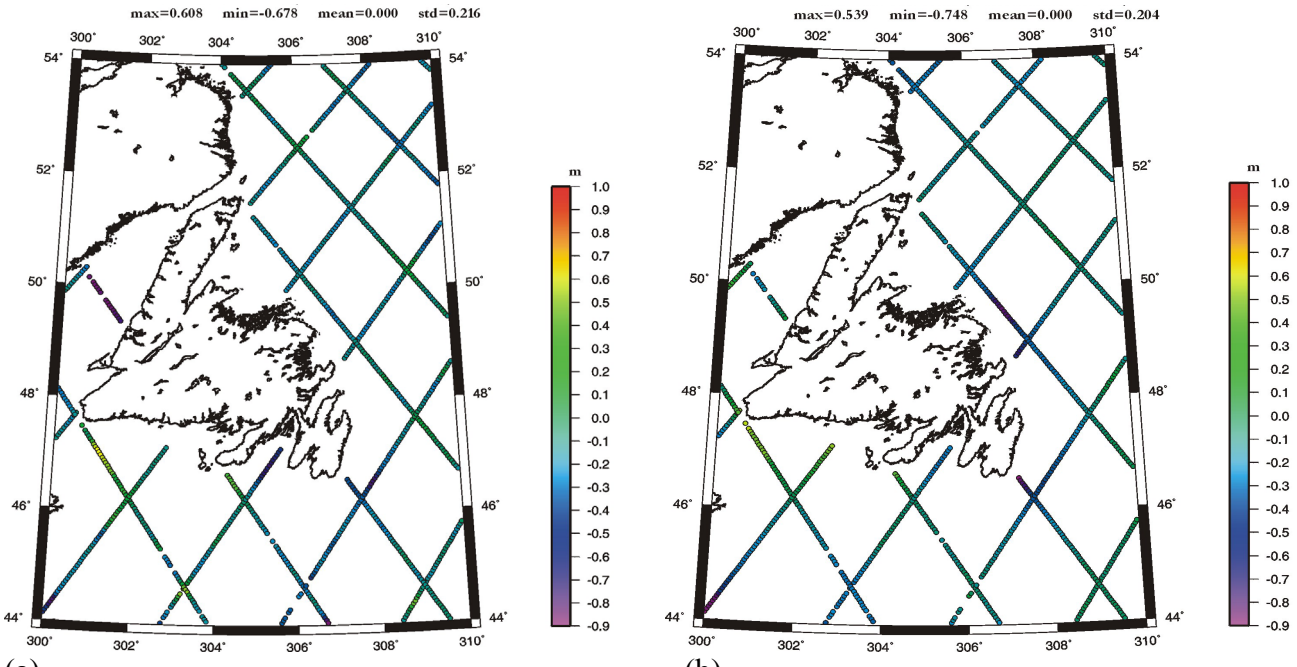

(a) (b)

Figure 11. Differences between the final geoid height solutions from the MIMOST method for EGM96 (a) and GPM98b (b) reference models and the stacked T/P SSHs (3rd year).

6. CONCLUSIONS – FUTURE PLANS

Eight local geoid solutions were computed for the Eastern part of Canada close to the island of Newfoundland in the Labrador Sea. We determined pure altimetric and gravimetric geoid height solutions for the area under study using two geopotential models, namely EGM96 and GPM98b, as reference fields. The MIMOST method for the optimal combination of heterogeneous data was then used to determine the final geoid solutions. Throughout this study the well-known remove-restore method is used for the geoid determination when the gravimetric residual geoid heights are computed using the 1-D spherical FFT method.

Based on these results the determination of a purely altimetric geoid is possible with an accuracy close to ±7cm while the determination of a purely gravimetric one has a lower accuracy close to ±20cm. The differences between T/P SSHs and the gravimetric geoid heights can be mainly attributed to the poorer accuracy of the available gravity data, at least compared to that of T/P SSHs. The differences between GSD95 and the ERS1-GM altimetric solution to EGM96 model are mainly due to the different reference fields used and to the more accurate data used in the present study.

As far as the combined solution is concerned, it is evident that the use of altimetry data, both for EGM96 and GPM98 reference fields, improves by ±3cm the accuracy of geoid determination as compared to the gravimetric only solution. This can be attributed not only to the more accurate altimetry data but to the noise level used for the different data sets (5cm for the altimetric and 10cm for the gravimetric ones) which give more weight to the altimetric geoid heights in the combination algorithm. The comparison of our combined solution with GSD95 gives better agreement close to the coastline when compared to the differences of the satellite only geoid models. This is an indication that the use of shipborne gravity data enhances the altimetric only solutions, since the later lack data close to the coastline and in shallow ocean areas. Throughout this research, GPM98b proved to give better or equal agreement, compared to EGM96, with our control datasets. This is an indication that it is more appropriate to use GPM98b as the reference field, at least for the test area, when geoid modeling is concerned.

A detailed study of the different solutions, with more emphasis on the error spectrum, and an investigation of the frequency contents of the two geopotential models is needed and will be carried out. Additionally special emphasis will be paid on the coastline when combining land and marine gravity data for geoid determination and towards the investigation for a numerical solution of the fixed Altimetry Gravimetry Boundary Value Problem (AGBVP). In order to obtain a higher resolution and higher accuracy geoid solution in the area under study, an improvement of the marine gravity databases is necessary.

Acknowledgements

The financial assistance provided to the first two of the authors by the GEOIDE Network of Centers of Excellence is gratefully acknowledged. We extensively used the Generic Mapping Tools Version 3.1 (Wessel and Smith, 1998) in displaying our results.

References

Andersen, O.B. and P.Knudsen. *Global marine gravity field from the ERS1 and GEOSAT geodetic mission altimetry*. J. Geophys. Res., Vol. 103, No. C4, pp. 8129 (97JC02189), 1998.

Andritsanos, V.D., M.G. Sideris and I.N. Tziavos. *A survey of gravity field modelling applications of the Input-Output System Theory (IOST)*. To appear in IGeS Bulletin, 2000a.

Andritsanos, V.D., M.G. Sideris and I.N. Tziavos. *Quasi-stationery Sea Surface topography estimation by the multiple Input-Output method*. Accepted for publication in Journal of Geodesy, 2000b.

AVISO User Handbook – Corrected Sea Surface Heights (CORSSHs). AVI-NT-011-311-CN, Edition 3.1, 1998.

Bendat, J.S. and Piersol A.G. *Random data: Analysis and Measurement Procedures*. Second edition. John Wiley and Sons, New York, 1986.

The Geosat Altimeter JGM-3 GDRs Handbook. Internet Resources:http://www.ibis.gdrl.noss.gov/SAT/gdrs/geosat-handbook, 1997.

Haagmans, R., E. de Min and M. van Gelderen. *Fast evaluation of convolution integrals on the sphere using 1D FFT, and a comparison with existing methods for Stokes' integral*. Manuscr. Geod. 18, pp. 227-241, 1993.

Li, J. *Detailed marine gravity field determination by combination of heterogeneous data*. UCGE Reports No. 20102, Department of Geomatics Engineering, The University of Calgary, Calgary, Alberta, Canada, 1996.

Lemoine, F.G., et al. *The development of the join NASA GSFC and NIMA geopotential model EGM96*, NASA Technical Paper, 1998 – 206861, 1998.

National Oceanographic and Atmospheric Administration - NOAA. *The GEOSAT-GM Altimeter JGM-3 GDRs*. 1997.

Sandwell D. *Data Base Description for Digital Bathymetric Data Base-Variable Resolution (DBDB-V)*. Version 1.0, Naval Oceanographic Office, Stennis Space Center, March, 1996.

Sideris, M.G. *On the use of heterogeneous noisy data in spectral gravity field modeling methods*. Journal of Geodesy, 70, pp. 470-479, 1996.

Sideris, M.G. and B.B. She. *A new high-resolution geoid for Canada and part of the U.S. by 1D-FFT method*. Bull. Geod. 69:92-108, 1995.

Smith, W.H.F. and D.T. Sandwell. *Bathymetric prediction from dense satellite altimetry and sparse shipboard bathymetry*. Journal of Geophysical Research, 99, No. B11, 21803-21824, 1994.

Vergos, G.S., *The contribution of satellite altimetry to gravity field modeling – A case of study in the Eastern Mediterranean*. Diploma thesis, School of Rural and Surveying Engineering, Faculty of Engineering, Aristotle University of Thessaloniki, Department of Geodesy and Surveying, 2000.

Véronneau, M. *Shipborne gravity data for the area of Newfoundland, Canada*. Gravity data from the Geological Survey of Canada, personal communication, 2001.

Véronneau, M. *The GSD95 Geoid Model for Canada*. Gravity Geoid and Marine Geodesy, Proceedings of international symposium, Tokyo, Japan, 1996. Springer Vol. 1997, pp. 573-580, 1997

Wenzel, H.G. *Global models of the gravity field of high and ultra-high resolution*. In Lecture Notes of IAG's Geoid School, Milano, Italy, 1999.

Wessel, P., and W.H.F. Smith. *New improved version of Generic Mapping Tools released*. EOS Trans. Amer. Geophys. U., vol. 79 (47), pp. 579, 1998.

Correspondence to: Georgios S. Vergos, Department of Geomatics Engineering, The University of Calgary, 2500 University Drive N.W., Calgary, Alberta, Canada, T2N 1N4, ++1 (403) 220-4113, **gsvergos@ucalgary.ca**